Journal of the European Ceramic Society **11** (1993) 325–333

Alumina Microstructural Behaviour under Pressureless Sintering and Hot-Pressing

J. F. Roy, M. Descemond, C. Brodhag & F. Thevenot

Ecole Nationale Supérieure des Mines, 158, cours Fauriel, 42023 Saint-Etienne Cédex, France

(Received 27 April 1992; revised version received 8 July 1992; accepted 15 July 1992)

Abstract

The aim of this study is to observe the microstructural evolution of a Bayer alumina as a function of different parameters under pressureless sintering and hot-pressing: soaking temperature, soaking time and applied pressure. Experiments indicate a preponderant contribution of the temperature on the microstructure control whatever the sintering mode may be.

A semi-manual technique of digitization of the microstructure using a digital tablet allows quantification of the size, the shape and the orientation of the grains. For both sintering modes and beyond a grain size threshold, increase of temperature leads to anisotropic grain growth of the coarser fraction at the expense of the finer fraction.

The pressure has an effect on the mobility of grain boundaries and contributes to an elongation that is similar for all the grains. Nevertheless the microstructures under high pressure produce a distribution of strongly elongated grains with an orientation perpendicular to the pressure axis.

Das Ziel dieser Arbeit ist die Untersuchung der mikrostrukturellen Entwicklung von Bayer-Aluminiumoxid als Funktion von Endtemperatur, isothermer Haltezeit und Druck bei drucklosem Sintern und Heißpressen. Die Experimente weisen bei beiden Sinterverfahren auf eine überwiegende Abhängigkeit der Mikrostruktur von der Temperatur hin.

Die halbmanuelle Digitizierung der Mikrostruktur mittels eines Digitizierungstabletts erlaubt die Quantifizierung von Größe, Form und Orientierung der Körner. Oberhalb einer Korngrößenschwelle bewirkt eine Temperaturerhöhung bei beiden Sinterverfahren ein bevorzugtes Kornwachstum der Grobkornfraktion auf Kosten der Feinkornfraktion.

Druck beeinflußt die Mobilität der Korngrenzen und trägt zu einem bei allen Körnern ähnlichen Längenwachstum bei. Unter hohem Druck weist die Mikrostruktur jedoch eine Verteilung von Körnern mit starkem Längenwachstum und einer Orientierung senkrecht zur Druckrichtung auf.

Le but ce cette étude est de suivre l'évolution des microstructures d'une alumine Bayer en fonction de différents paramètres lors d'un cycle de frittage naturel ou sous pression: température de palier, temps de palier et pression appliquée. Les expériences sélectionées à partir de la méthodologie de la recherche expérimentale mettent en évidence l'effet prépondérant de la température sur le contrôle de la microstructure et ceci quel que soit le mode de frittage utilisé.

Une technique semi-manuelle de digitalisation des microstructures composée d'une table à digitaliser permet de quantifier la taille des grains, leur forme ainsi que leur orientation préférentielle. Pour les deux modes de frittage et au-dessus d'une taille moyenne de grains, l'accroissement de température conduit à un grossissement anisotrope des gros grains aux dépens des petits.

La pression en jouant sur la mobilité des joints de grains permet une élongation assez homogène de tous les grains. Cependant les microstructures issues d'un frittage sous forte pression révèlent une distribution de grains fortement allongés orientés perpendiculairement à l'axe de pression.

1 Introduction

The sintering of alumina is due to several mechanisms like surface or volume diffusion. These mechisms allow reduction in the interface energy of the system and they can occur simultaneously to control the density and to produce normal or abnormal grain growth depending on the stage of sintering.

Models exist which try to explain ceramic behavior in the intermediate and final stages of sintering[1] but particle shape variations,[2,3] influenced by either impurity levels[4] or additives,[5–7] are

Journal of the European Ceramic Society 0955-2219/93/$6.00

commonly ignored. The influence of the γ–α phase ratio in pure aluminas on crystal growth has been determined.[8]

The aim of this study is to follow the microstructural evolution in terms of different parameters under pressureless sintering and hot-pressing—soaking temperature, soaking time and applied pressure—using a specific methodology of research.

A quantitative technique using a digital tablet and scanning electron microscope photographs provides a basis on which to characterize different kinds of microstructures including factors such as Al_2O_3 grain size, shape and preferred orientation.

By comparison between sintering and pressure-sintering, the influence of pressure on the microstructure can be estimated.

2 Experimental

The alumina powder used (P172SB, Pechiney, France) is described in Table 1. The starting powders used for pressureless sintering are cold isostatically pressed under 400 MPa (green density from 58·6% to 60·9%). A methodology developed by Phan-Tan-Luu and coworkers[9] consists of describing the studied phenomenon, i.e. finding the relations between the factors (in this study, the sintering parameters) and the responses (here, density and grain size). The results are processed by the exploitation software NEMROD[10] using mathematical models.

A classical method consists in changing only one parameter and in measuring the response for different values of this parameter. The methodology used in this study differs from the classical method since all the parameters vary simultaneously in a programmed and rational way for each experiment. The parameter values are determined from acquired knowledge about the system (bibliography, earlier experiences, etc.); a domain for the interpretation of results is defined. The quality of interpretation depends on the selected domain.

The results for pressureless sintering are given in a second degree polynomial,[11] the two parameters being soaking temperature and soaking time; the experimental points are defined in Fig. 1(a). The results for hot-pressing are given in a first degree polynomial;[12,13] the three parameters are soaking temperature, soaking time and applied pressure (Fig. 1(b)). The aim of this study is to appreciate the pressure effect on the microstructure.

The hot-pressing cycles are described in Fig. 2. The equipment used is a laboratory press, type

Table 1. Specifications of the P172SB alumina powder

Process		Bayer
Powder		P172SB
Producer		Pechiney, France
Specific surface (m^2/g)		10·3
Mean diameter D_{50} (μm)		0·45
Impurity (ppm)	Fe	161
	Na	237
	Si	443
	Ca	250
	Mg	660
Green density (at 352 MPa)		2·20

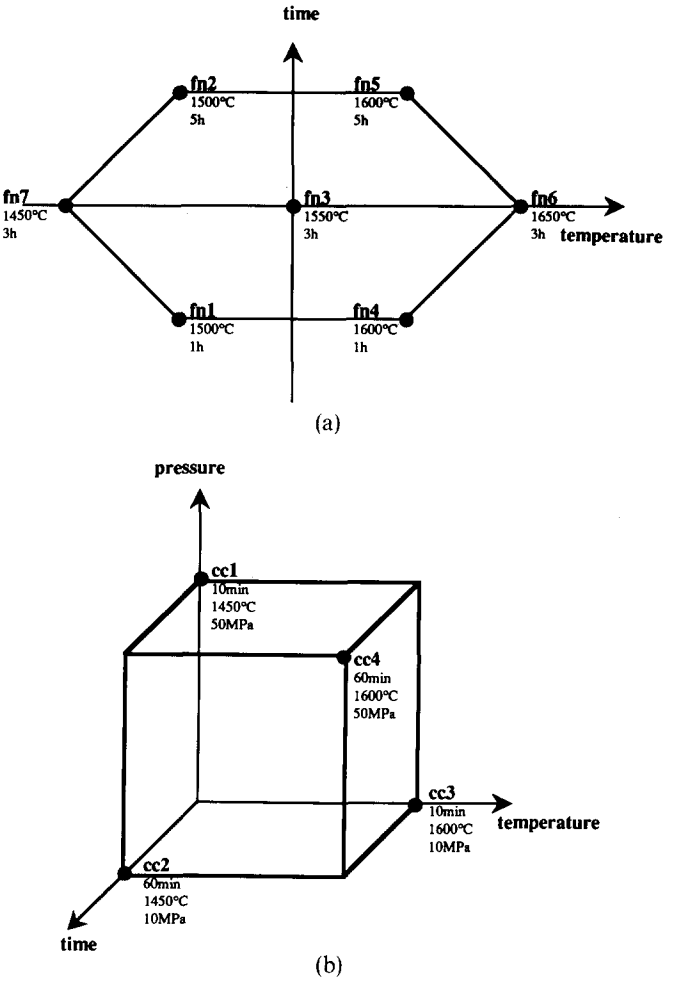

Fig. 1. Experimental points for (a) pressureless sintered and (b) hot-pressed samples.

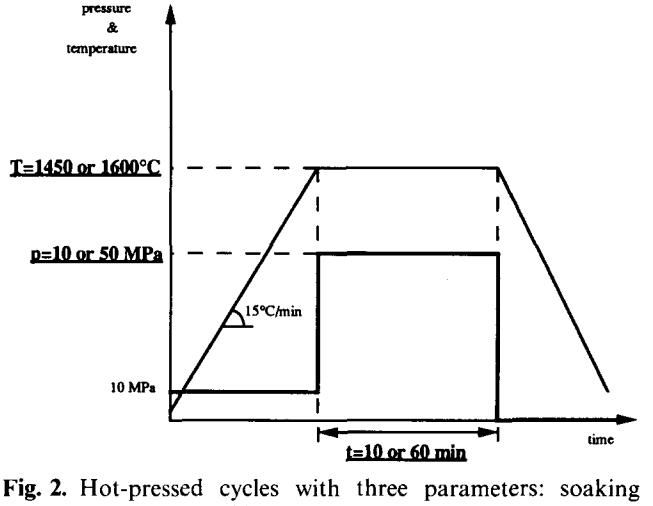

Fig. 2. Hot-pressed cycles with three parameters: soaking temperature (T), soaking time (t) and applied pressure (p).

Table 2. Description and characterization of experiments (fn = pressureless sintering, cc = hot-pressing)

	Time (*h*)	*Temperature* (°C)	*Pressure* (*MPa*)	*Density* (%)	D_{10} (μm)	D_{50} (μm)	D_{90} (μm)	*Percentage of elongated grains*
Initial powder	—	—	—	—	0·14	0·45	0·88	—
fn1	1	1 500	—	96·3	0·42	0·83	1·72	11
fn2	5	1 500	—	98·1	0·54	1·04	2·18	14
fn3	3	1 550	—	98·7	0·72	1·31	2·66	14
fn4	1	1 600	—	98·9	0·92	1·84	4·33	15
fn5	5	1 600	—	98·7	1·39	2·84	8·80	24
fn6	3	1 650	—	98·5	1·70	3·90	11·49	25
fn7	3	1 450	—	93·4	—	—	—	—
cc1	10 min	1 450	50	99·4	0·47	0·90	1·91	16
cc2	1	1 450	10	99·3	0·46	0·92	2·01	14
cc3	10 min	1 600	10	98·9	0·96	2·02	5·26	22
cc4	1	1 600	50	99·5	1·40	3·63	10·50	25

GOLIATH-LPA (France). The temperature limit of the graphite resistor is 2200°C. Forces can be developed up to 100 kN. The inner diameter of the graphite die is 50 mm, so a pressure of 50 MPa can be reached. The working atmosphere is vacuum (less than 9×10^{-4} mb). Densities of the resulting ceramic cylinders are determined by the Archimedes technique in water (Table 2). The sintered samples are cut with a diamond saw and the observed faces are parallel to the pressure axis. These faces are carefully polished down to 3 μm with diamond paste. The grain boundaries are revealed by thermal etching in air for 1 h at 1450°C.

Back-scattered electron images are not sufficiently well defined for direct image analysis. A semi-manual technique developed by Brodhag and coworkers[8,14] for digitizing the microstructure is used. A photograph (scale approximately × 1000) is placed on a digitizing tablet (Hitachi IIIB) connected to a personal computer (IBM PC). The position and the dimensions of each grain are measured using two diameters (Fig. 3). A grain is considered elongated when its anisotropy or elongation factor is larger than 2. The centre coordinates of each grain and the mean diameter, average of the two measured diameters, are kept in the memory. The final data file contains, for each phase, the results of different photographs for up to a thousand grains, which is the minimum to avoid statistical bias. The grain size distribution based on the number of particles is calculated. Assuming a spherical shape, the apparent diameter observed on the surface is multiplied by $4/\pi$ to approximate the real diameter.

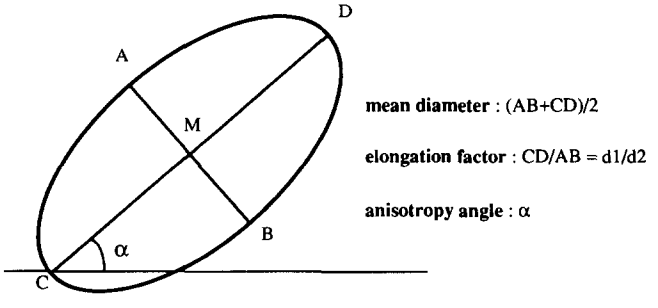

Fig. 3. Data collected during manual digitizing operation.

To characterize the distribution the median grain size D_{50} is used, for which 50% (number percentage) of the grains are smaller than this value in microns (Fig. 4). Similarly, D_{10} and D_{90} can be defined, D_{10} representing the size of the finer fraction of the grains and D_{90} the coarser fraction. The evolution of elongation factor versus grain size is represented in a topological form (Fig. 5). Finally, this digitizing technique makes some details clear about the orientation of elongated grains. One representation gives the number of elongated grains versus oriented grain angle (Fig. 6) and two representations, both in a topological function, give grain size versus anisotropy angle (Fig. 7(a) and (b)) and elongation factor versus anisotropy angle (Fig. 7(c) and (d)).

3 Results

3.1 Densification rate

Table 2 confirms that the highest densities occur as expected under hot-pressing, notwithstanding the fact that the sintering time is shorter. Pressure

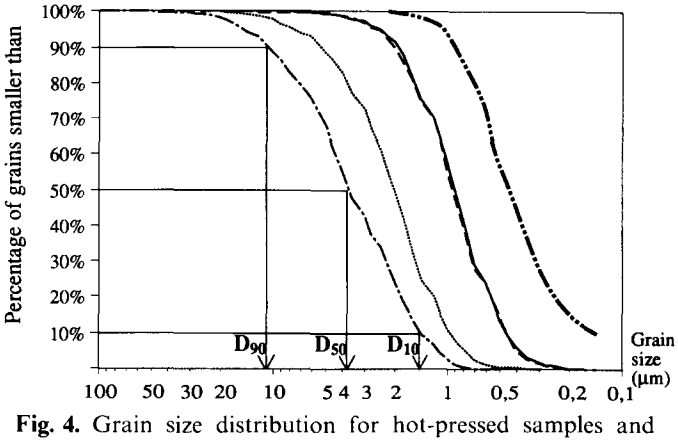

Fig. 4. Grain size distribution for hot-pressed samples and definition of D_{10}, D_{50} and D_{90}. —·—, Initial powder; ——, cc1; – – –, cc2; ·····, cc3; —··—, cc4.

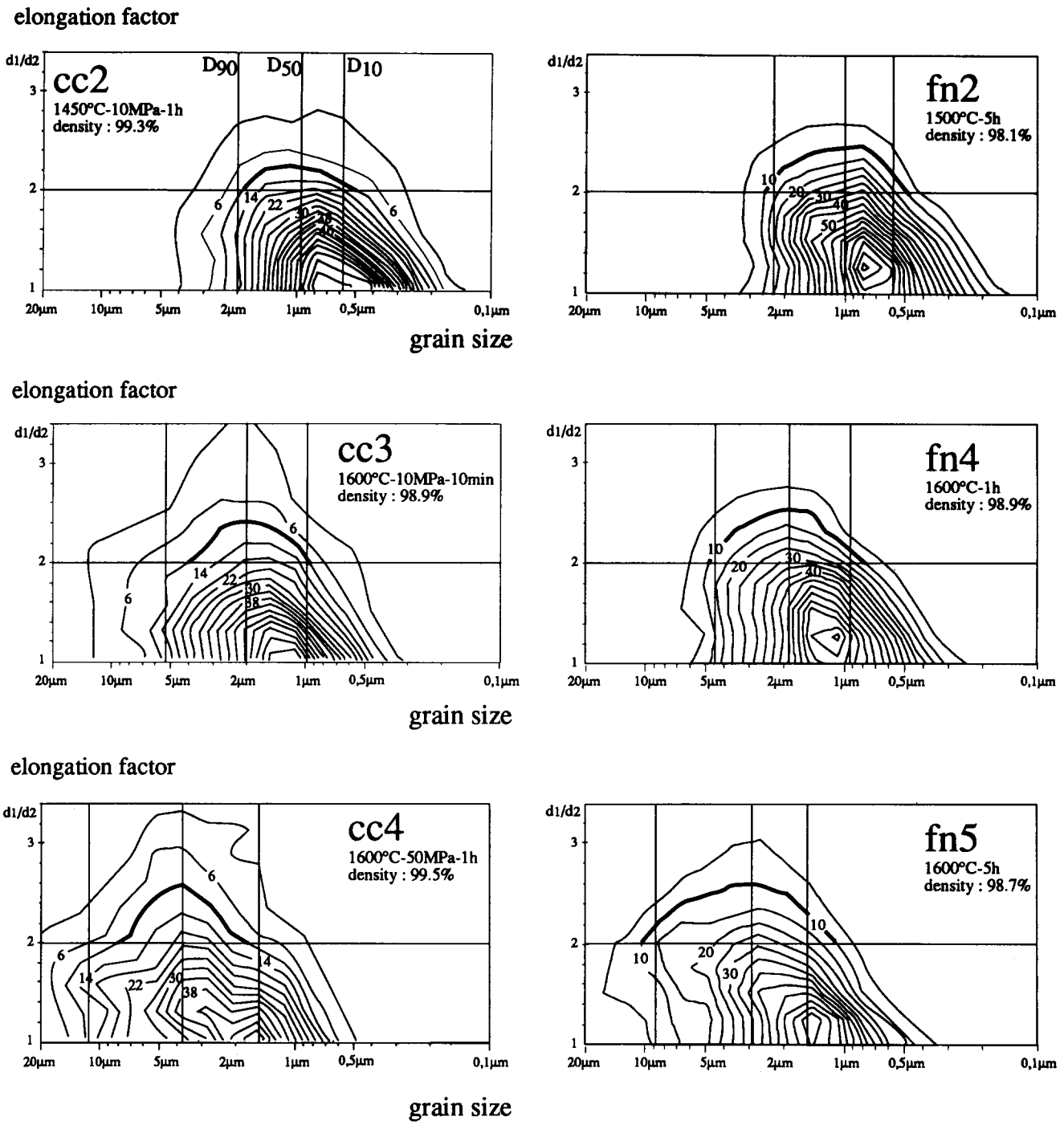

Fig. 5. Microstructural topographic curves.

'accelerates' sintering: 99% of theoretical density is obtained under either a sintering cycle (1600°C, 1 h) or a hot-pressing cycle (1600°C, 10 min, 10 MPa) (Fig. 8).

The results for the pressureless sintering densities allow isodensity curves to be plotted into the experimental domain (Fig. 9). This figure shows an increase of the densification rate with temperature and soaking time up to 1600°C. Beyond this temperature a 'dedensification' occurs with an exaggerated effect for long soaking times.[15] Some authors justify this 'dedensification' by the elimination of adsorbed gas on the powder surface[16] and by oxidation of carbonaceous impurities.[17] Other authors interpret this 'dedensification' as a result of the diminution of the free interface energy by pore formation[18] with simultaneous formation of faceted interfaces.

The density results from hot-pressing experiments are summarized in Fig. 10. If the polynomial degree is adequate, the density value ρ_0 would be the density of a sample defined by all the factors at a mean level; in the present case an experiment realized at a temperature of 1525°C, a soaking time of 35 min and an applied pressure of 30 MPa. For a given response, the weight factor value $\delta\rho_p$ for example is equal to the density gap between the ρ_0 value and the sample value ρ, with the pressure

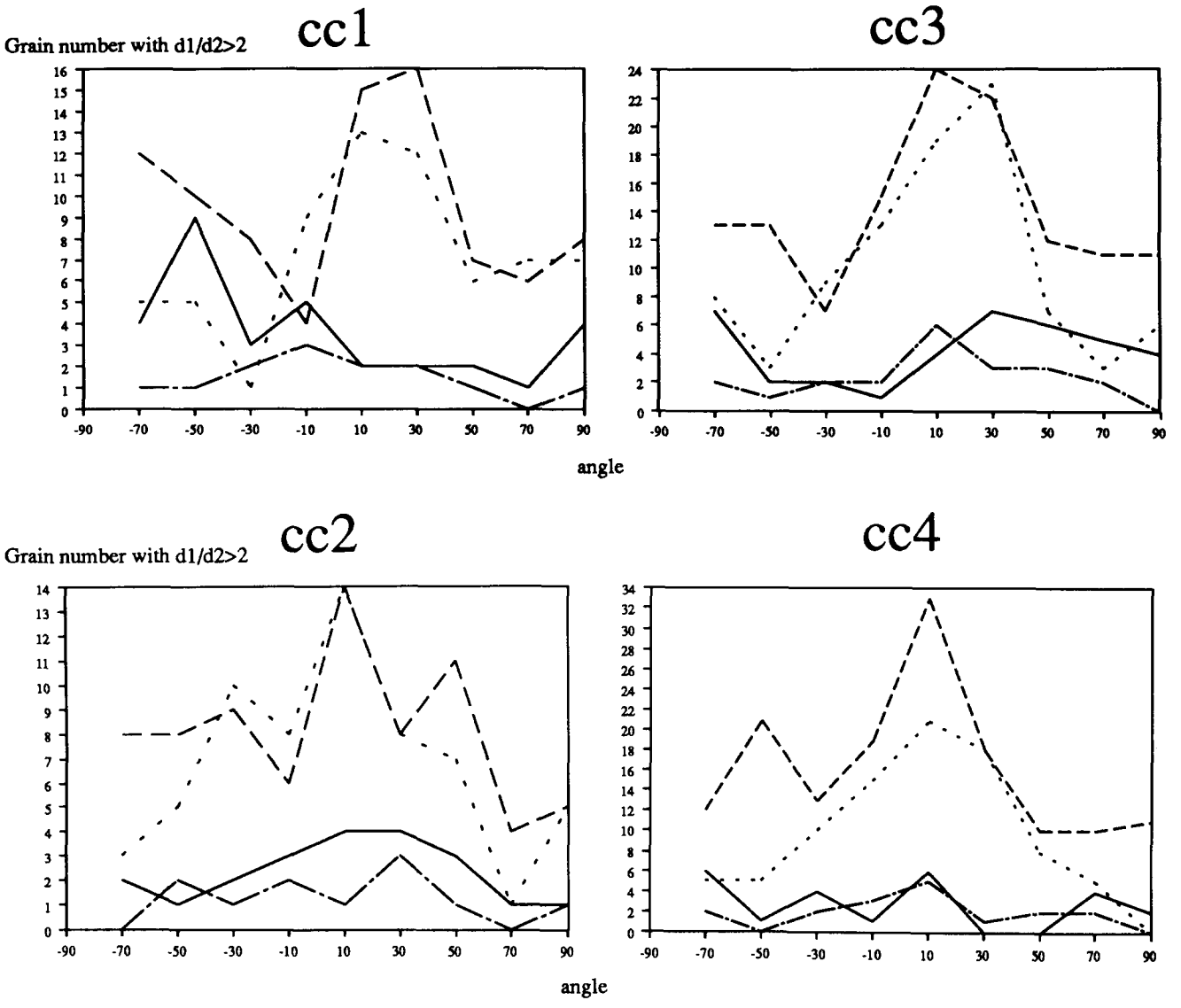

Fig. 6. Elongated grain number per size fraction as a function of anisotropy angle for hot-pressed samples. ——, $D_{10} > D$ (finer fraction); – – –, $D_{50} > D > D_{10}$; ·····, $D_{90} > D > D_{50}$; — · —, $D > D_{90}$ (coarser fraction).

factor at a high level (all other factors at their mean levels); in other words the variation of pressure from 30 to 50 MPa represents a density improvement of 0·17% from ρ_0 (with $T = 1525°C$ and $t = 35$ min). Density is improved by high pressure ($\delta\rho_p > 0$) and long soaking time ($\delta\rho_t > 0$). It can be seen that a temperature increase from 1525°C to 1600°C (with $p = 30$ MPa and $t = 35$ min) reduces the density value ρ_0 from 99·28 to $\rho_0 + \delta\rho_T = 99{\cdot}20\%$. The $\delta\rho_T$ value is an average variation from a short to a long soaking time. The $\delta\rho_T$ negative value can be explained in the following manner: the passage from 1450°C to 1600°C with a short soaking time is followed by a drop in density, due to the selected pressure conditions—much lower at 1600°C than at 1450°C. This density diminution is not necessarily the consequence of a 'dedensification' at 1600°C but instead of a low applied pressure at this temperature. It is noted that a time and pressure increase (cumulative effect) does not lead to a drop in density (Fig. 11). In the same way, a temperature and time increase (at constant pressure) does not change the density (Fig. 11).

3.2 Microstructure

Whereas the density increases with temperature, the grain growth represented by the D_{50} mean size only starts at 1550°C and increases with temperature. In the case of pressureless sintering a threshold temperature T[15] can be characterized as follows:

—If $T \leq 1550°C$, then an increase in temperature and time involves an increase in density without grain growth (D_{50} about 1 μm).

—If $T > 1600°C$, then an increase in both these parameters leads to grain growth. The time effect is significant (Fig. 8) when fn4 and fn5 (fn = pressureless sintering) are compared: the mean grain size increases with time at 1600°C.

In the case of hot-pressing, grain growth is mainly controlled by temperature in the range 1450–1600°C; indeed a temperature increase from

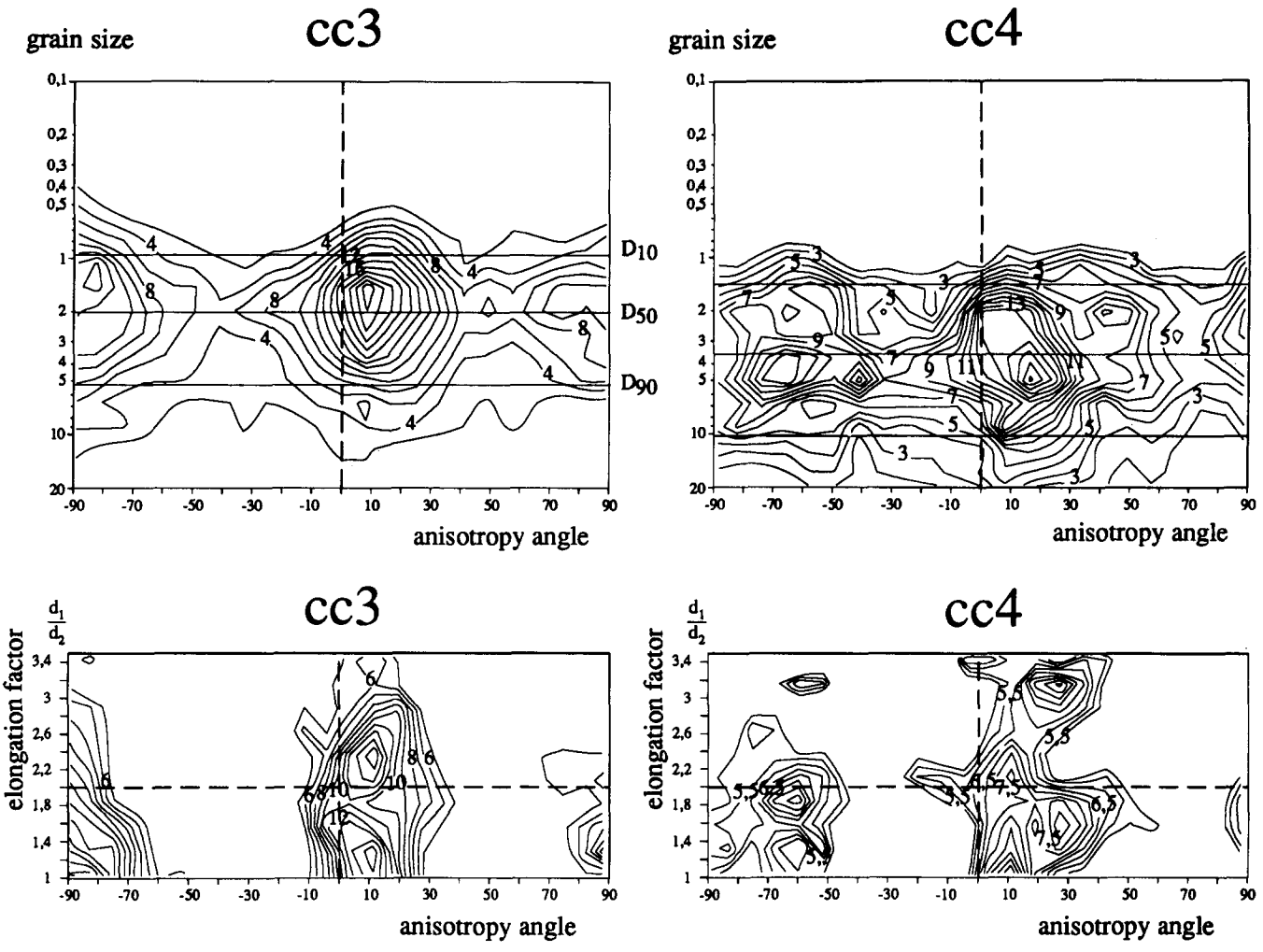

Fig. 7. Microstructural topographic curves for hot-pressed samples.

1525°C to 1600°C (with $p = 30$ MPa and $t = 35$ min) results in a D_{50} increase from $D_0 = 1{\cdot}87\,\mu$m to $D_0 + \delta D_T = 2{\cdot}83\,\mu$m according to the results of the polynomial model (Fig. 12). The effects of soaking time and pressure are also favourable to grain growth but these effects are less important.

It is pointed out that the D_{50} evolution gives only global information about microstructure growth; this evolution does not include such effects as an abnormal growth (anisotropic growth for example).

3.3 'Non-classical' grain growth

When normal growth occurs, the whole microstructure evolves similarly; in particular both the D_{10}/D_{50} and D_{90}/D_{50} ratios are almost constant for one type

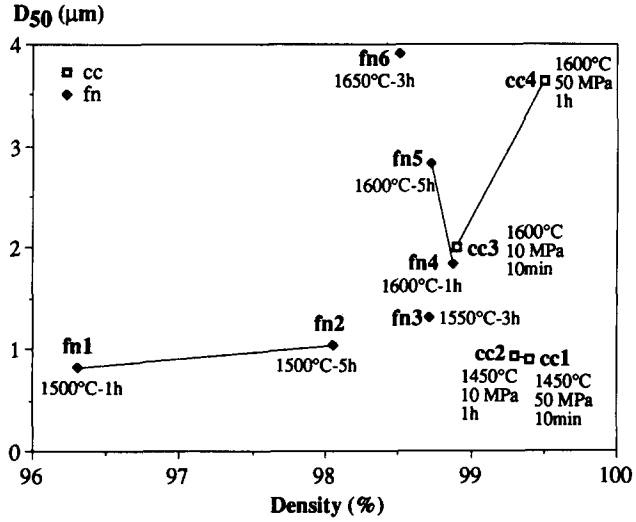

Fig. 8. Evolution of the median grain size D_{50} as a function of relative density.

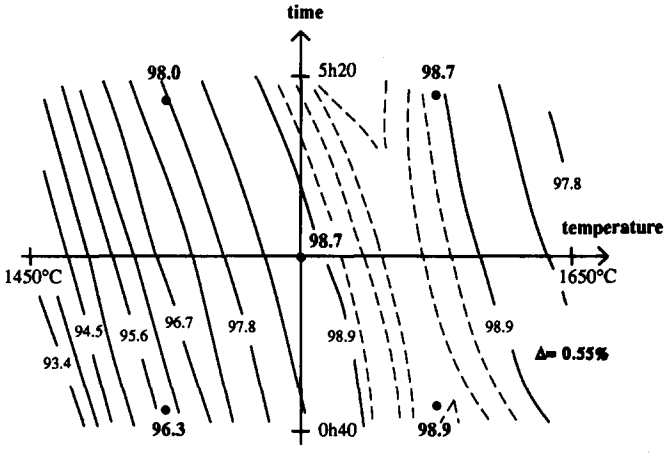

Fig. 9. Isodensity curves under pressureless sintering. $D = -576{\cdot}94 - 862{\cdot}52 \times 10^{-3}\,T - 696{\cdot}69 \times 10^{-2}\,t - 275{\cdot}5 \times 10^{-6}\,T^2 - 784{\cdot}56 \times 10^{-5}\,t^2 + 465{\cdot}1 \times 10^{-5}\,Tt$.

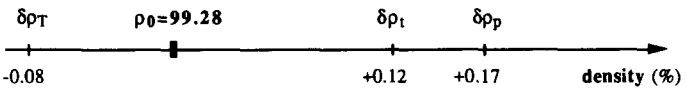

Fig. 10. Parameters effect on density for hot-pressed samples.

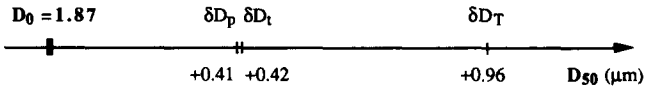

Fig. 12. Parameters effect on the mean size for hot-pressed samples.

of product. In other words, a normal growth leads to a perfect superposition of size distribution curves by simple translation; for example, both cc3 and cc4 (cc = hot-pressing) samples involve an abnormal grain growth under hot-pressing (Fig. 4); cc1 and cc2 samples have size distribution curves narrower than cc3 and cc4, the latter two samples having an obvious grain coarsening for larger grains, near D_{90}.

It is interesting to compare the microstructures obtained by pressureless and hot-pressing in particular to collect quantitative information about normal and abnormal grain growth. The comparison of D_{90}/D_{50} and D_{10}/D_{50} ratios allows the determination of a temperature threshold (Fig. 13); sintering conditions for cc3, cc4, fn4, fn5 and fn6 samples (with $T > 1550°C$) promote the grain growth of coarser grains more than that of finer grains. Microstructures from cc1, cc2, fn1, fn2 and fn3 samples ($T < 1550°C$) represent a narrower size distribution with a non-exaggerated grain growth of the coarser fraction (Fig. 13).

It has been shown that a high temperature ($T > 1600°C$) contributes to the grain growth D_{50}. On the one hand, microstructures with a D_{50} value lower than 2 μm present a normal growth (D_{90}/D_{50} ratio is near that of the starting powder). On the other hand, microstructures with a D_{50} value larger than 2 μm show an exaggerated grain growth of the coarser fraction (D_{90}/D_{50} ratio is increased and the D_{10}/D_{50} ratio is near that of the initial powder). In that case microstructures have abnormal grain growth with the disappearance of the finer fraction to the benefit of the coarser fraction.

These observations are valid for both sinterings; in fact, for pressureless sintering, the abnormal grain growth is a little greater for a high temperature and for a long soaking time. So it can be estimated that a threshold grain size allows the passage from quasi-normal to abnormal grain growth (Fig. 13).

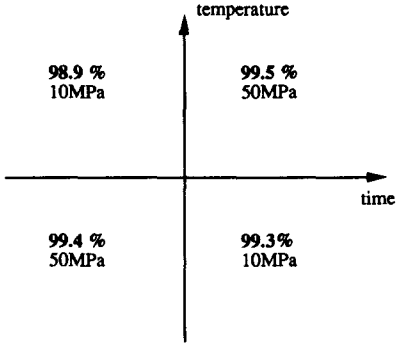

Fig. 11. Temperature effect on density for hot-pressed samples.

In hot-pressing, the methodology results for the D_{90}/D_{50} and D_{10}/D_{50} ratios allow the accurate characterization of this abnormal grain growth (Fig. 14). Temperature, soaking time and pressure increase lead to grain growth of the coarser fraction but not of the finer one. It can be seen that neither the D_{90}/D_{50} ratio nor the D_{10}/D_{50} ratio gives any indications about the grain shape, since these ratio values are mean diameters (AB + CD)/2 (Fig. 3).

3.4 Grain preferential elongation

According to Table 2, the percentage of elongated grains increases with temperature for both types of sintering. This is linked to a grain growth at a temperature above 1550°C in particular.

With pressureless sintering and with temperatures under 1550°C, the time increase has little influence on the percentage of elongated grains. Beyond 1550°C, the abnormal grain growth is characterized by an elongation, which affects an increasing fraction of grains as the soaking time increases (Table 2, fn4 and fn5).

Under hot-pressing at 1600°C (or 1450°C), time and pressure increase have little influence on the percentage of elongated grains (the values available in Table 2). The percentage of elongated grains per size fraction under hot-pressing (Table 3) exhibits an

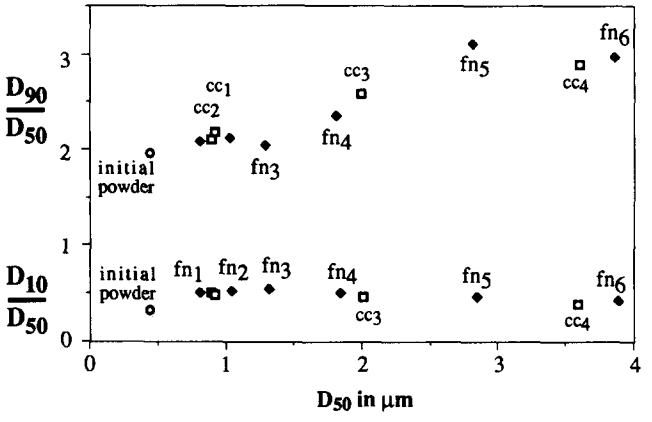

Fig. 13. Grain growth evolution under both (◆) pressureless sintering and (□) hot-pressing.

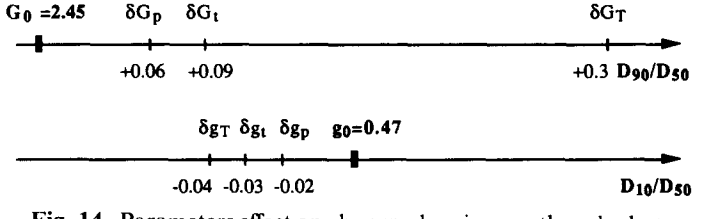

Fig. 14. Parameters effect on abnormal grain growth under hot-pressing.

Table 3. Elongated grain percentage per size fraction under hot-pressing

	Elongated grain percentage (CD/AB > 2) per size fraction			
	cc1	*cc2*	*cc3*	*cc4*
$D_{10} > D$ (finer fraction)	5·0	4·4	9·7	6·2
$D_{50} > D > D_{10}$	13·3	10·6	16·9	23·0
$D_{90} > D > D_{50}$	17·9	16·5	26·7	31·1
$D > D_{90}$ (coarser fraction)	28·4	26·0	31·7	31·5

important elongated grain percentage for the coarser fraction ($D > D_{50}$); on the other hand, the elongated grain percentage for the finer fraction is limited. These indications are confirmed for all microstructures under hot-pressing and they are emphasized at high temperatures. So there is a clear relationship between grain growth and elongated grains.

The values printed on the topological curves (Fig. 5) correspond to the number percentage of grains lying outside the boundary defined by these curves. In other words, the cc2 topological function, for example, indicates that 4% of grains are located between two consecutive curves. A homogeneous microstructure exhibits concentric topological curves and anisotropic factors less than 2 (see Fig. 3). In contrast, the distorted curves give indications about abnormal grain growth.

The cc2 sample, compared with the fn2 sample (Fig. 5), has a higher density value, an identical value of total elongated grain number and a smaller elongated factor for both the mean and the coarser fraction.

It has been noticed that under hot-pressing, the grain elongation was exaggerated for grain sizes larger than D_{50}. In fact this phenomenon is emphasized even more for pressureless sintering. The pressure, probably operating on the grain boundary mobility, makes densification easier and allows abnormal growth to start for more scattered grain sizes (Fig. 5).

Two other comparisons give support to this idea: the cc3 sample, compared with the fn4 sample (Fig. 5), has the same density value, a higher mean diameter D_{50} (2·02 μm compared to 1·84 μm) with more numerous elongated grains (22% compared to 15%) but with more scatter in the different grain sizes and with less elongated grains in the coarser fraction (Table 2). The cc4 sample, compared with the fn5 sample (Fig. 5), has the same sintering temperature (1600°C), a higher density value (99·5% compared to 98·7%), a higher mean diameter value D_{50} (3·63 μm and compared to 2·84 μm), and almost the same elongated grain percentage (Table 2), elongated grains being equally distributed in every size fractions (Table 3, see cc4).

3.5 Preferential grain orientation in hot-pressing

A graphic representation (Fig. 6) gives the number of elongated grains per size fraction versus the anisotropic angle. A preferential orientation (perpendicular to the pressure axis) can be observed for the mean fraction ($D_{10} < D < D_{90}$) in any of the microstructures; a liquid phase could allow this orientation.[19,20] In contrast, the coarser fraction allows a majority of elongated grains (Table 3) but without obvious preferential orientation. The finer fraction ($< D_{10}$) contains few or no oriented grains. The elongated and oriented grains increase in number with temperature.

The topological curves (Fig. 7) confirm the well-defined orientation of the mean fraction for the cc3 microstructure: in fact the cc3 elongated grains ($d_1/d_2 > 2$) have a preferential grain orientation between 0 and 20 degrees (Fig. 7(c)) and this orientation affects the mean fraction of grains more (summit for an anisotropic angle close to 0 and a diameter close to D_{50} from Fig. 7(a)). On the other hand, the cc4 microstructure presents two kinds of population: oriented grains (perpendicular to the pressure axis) with an elongated ratio of about 3 and less oriented grains with an elongated ratio of about

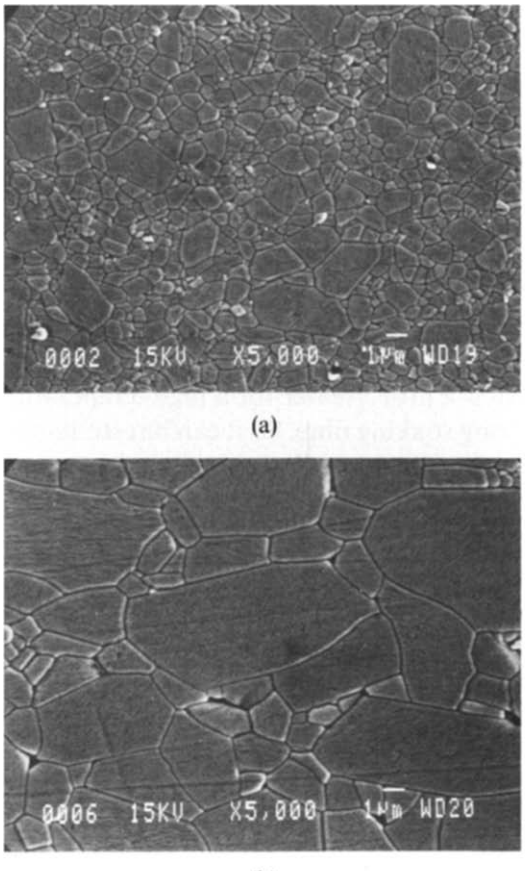

Fig. 15. Micrographs of hot-pressed samples (a) cc1 (1450°C, 50 MPa, 10 min) and (b) cc3 (1600°C, 10 MPa, 10 min).

2 (Fig. 7(d)). The pressure and soaking time increase at 1600°C leads to grains which are not more oriented but which have a higher elongated ratio ($d_1/d_2 > 3$).

3.6 Micrographs

For density varying from 98·9 (cc3) to 99·4% (cc1), abnormal grain growth is observed, illustrating the influence of a high temperature (Fig. 15). When some large grains appear, it is difficult to select representative fields for quantitative analysis; so, for each phase, the final data file contains up to a thousand grains.

4 Conclusion

For both sinterings, temperature influences the microstructure. Temperature increase for temperature values less than 1550°C involves density increase with little or no grain growth. For temperature values higher than 1550°C, the major mechanism is grain growth.

For both sinterings, it can be estimated that a threshold grain size (2 μm) allows the passage from a quasi-normal to an abnormal grain growth with the disappearance of the finer fraction to the benefit of the coarser fraction. This proves the importance of the range of the grain distribution of the starting powder on the microstructure homogeneity.

With pressureless sintering a 'dedensification' is observed at and above 1600°C. The abnormal (anisotropic) grain growth mostly concerns the coarser grain fraction (above D_{50}). Microstructures under high pressure present elongated and oriented grains perpendicular to the pressure axis.

References

1. Shaw, N. J., Densification and coarsening during solid state sintering of ceramics: a review of the models. *Powder Metall. Int.*, **21** (1989) 25–9.
2. Harmer, M. P., Bennison, S. J. & Narayan, C., Microstructural characterization of abnormal grain growth development in Al_2O_3. *Mater. Sci. Res.*, **15** (1983) 309–20.
3. Song, H. & Coble, R. L., Morphology of platelike abnormal grains in liquid-phase-sintered alumina. *J. Am. Ceram. Soc.*, **73** (1990) 2086–90.
4. Handwerker, C. A., Morris, P. A. & Coble, R. L., Effects of chemical inhomogeneities on grain growth and microstructure in Al_2O_3. *J. Am. Ceram. Soc.*, **72** (1989) 130–6.
5. Bennison, S. J. & Harmer, M. P., Effect of MgO solute on the kinetics of grain growth. *J. Am. Ceram. Soc.*, **66** (1983) C-90–C-92.
6. Harmer, M. & Brook, R. J., The effect of MgO additions on the kinetics of hot pressing in Al_2O_3. *J. Mater. Sci.*, **15** (1980) 3017–24.
7. Harmer, M. P., Use of solid-solution additives in ceramic processing. *Advances in Ceramics*, **10** (1984) 679–96.
8. Descemond, M., Brodhag, C. & Thevenot, F., Quantitative microstructure evaluation: correlation with processing of alumina. In *Proc. 11th Riso International Symposium on Metallurgy and Materials Science: Structural Ceramics—Processing, Microstructure and Properties*, ed. J. J. Bentzen. Riso National Laboratory, Denmark, 1990, pp. 237–42.
9. Mathieu, D., Phan-Tan-Luu, R. & Feneuille, D., Méthodologie de la recherche expérimentale. LPRAI, Université d'Aix-Marseille III, France, 1980.
10. Mathieu, D. & Phan-Tan-Luu, R., Logiciel NEMROD. LPRAI, Université d'Aix-Marseille III, France, 1989.
11. Phan-Tan-Luu, R., Feneuille, D. & Mathieu, D., Méthodologie de la recherche expérimentale—etude des surfaces de réponses. Chap. III-D, Aix-en-Provence, 1983.
12. Phan-Tan-Luu, R., Feneuille, D. & Mathieu, D., Méthodologie de la recherche expérimentale—etude des surfaces de réponses. Chap. II, Aix-en-Provence, 1983.
13. Goupy, J., La méthode des plans d'expériences—optimisation du choix des essais et de l'interprétation des résultats. Chap. 5, Ed. Dunod, 1988.
14. Brodhag, C., Bach, J. P., Thevenot, F. & Deletter, M., Microstructure of zirconia-toughened alumina obtained through different precursor routes. *Mater. Sci. Eng.*, **A109** (1989) 53–9.
15. Descemond, M., Frittage et évolution microstructurale de céramiques de type oxyde—application à l'alumine et à la zircone yttriée. Thèse, INPG, ENSMSE, Saint-Etienne, France, 1991.
16. Rice, R. W., Fabrication and characterization of hot-pressed Al_2O_3. Naval Research Laboratory, Washington, DC, AD-709 556, 1970.
17. Bennison, S. J. & Harmer, M. P., Swelling of hot-pressed alumina. *J. Am. Ceram. Soc.*, **68** (1985) 591–7.
18. Rodel, J. & Glaeser, A. M., Anisotropy of grain growth in alumina. *J. Am. Ceram. Soc.*, **73** (1990) 3292–301.
19. Song, H. & Coble, R. L., Origin and growth kinetics of platelike abnormal in liquid-phase-sintered alumina. *J. Am. Ceram. Soc.*, **73** (1990) 2077–85.
20. Kaysser, W. A., Sprissler, M., Handwerker, C. A. & Blendell, J. E., Effect of a liquid phase on the morphology of grain growth in alumina. *J. Am. Ceram. Soc.*, **70** (1987) 339–43.